Constitutively active H-ras accelerates multiple forms of plasticity in developing visual cortex

Megumi Kaneko[a,1], Claire E. Cheetham[b,1], Yong-Seok Lee[c], Alcino J. Silva[c], Michael P. Stryker[a,2], and Kevin Fox[b]

[a]Department of Physiology and the Keck Center for Integrative Neurosciences, University of California, San Francisco, CA 94143-0444; [b]School of Biosciences, Cardiff University, Cardiff CF10 3AX, United Kingdom; and [c]Departments of Neurobiology, Psychiatry, and Psychology and Brain Research Institute, University of California, Los Angeles, CA 90095-1761

Contributed by Michael P. Stryker, September 16, 2010 (sent for review August 27, 2010)

Experience-dependent cortical plasticity has been studied by using loss-of-function methods. Here, we take the complementary approach of using a genetic gain-of-function that enhances plasticity. We show that a constitutively active form of H-ras (H-ras^{G12V}), expressed presynaptically at excitatory synapses in mice, accelerates and enhances multiple, mechanistically distinct forms of plasticity in the developing visual cortex. In vivo, H-ras^{G12V} not only increased the rate of ocular dominance change in response to monocular deprivation (MD), but also accelerated recovery from deprivation by reverse occlusion. In vitro, H-ras^{G12V} expression decreased baseline presynaptic release probability and enhanced presynaptically expressed long-term potentiation (LTP). H-ras^{G12V} expression also accelerated the increase following MD in the frequency of miniature excitatory potentials, mirroring accelerated plasticity in vivo. These findings demonstrate accelerated neocortical plasticity, which offers an avenue toward future therapies for many neurological and neuropsychiatric disorders.

gain of function | monocular deprivation | mouse | ocular dominance | presynaptic long-term potentiation

Synaptic plasticity plays important roles both in the establishment of neuronal connections during development and in adaptation of neuronal circuits to changes in sensory experience in later life (1, 2). In the visual system, a change in the balance of input from the two eyes alters synaptic connections in the binocular visual cortex (3, 4). The sensitivity of the visual cortex to change is at its peak during a developmental time window or "critical period" (5, 6). At this stage of development, closure of one eye (monocular deprivation; MD) causes neurons in visual cortex to decrease their responsiveness to the closed eye and increase their responsiveness to the open eye (7–10).

Neurons in the binocular zone of mouse primary visual cortex (V1) receive varying levels of input from the two eyes, but most neurons show a contralateral bias (10–12). During the critical period, the changes in responsiveness to the two eyes induced by MD take place in two mechanistically and temporally distinct phases. The first change is a decrease in responsiveness to the closed eye, which relies on an LTD-like mechanism (7, 9, 13). In contrast, the subsequent increase in open-eye responsiveness involves a homeostatic mechanism (9, 10). Recovery of normal visual responsiveness after MD is reversed engages yet another distinct mechanism, requiring TrkB kinase activity for recovery of both contralateral and ipsilateral eye responses (8).

A number of manipulations have been shown to impair plasticity or to alter the timing of the critical period (5), but it has not been possible to accelerate plasticity when it is at its peak. Adult mice expressing a constitutively active form of H-ras (H-ras^{G12V}) from the calcium/calmodulin-dependent kinase type IIα (CaMKIIα) promoter exhibit enhanced spatial learning and contextual fear conditioning, and have greater plasticity in the hippocampus (14). We studied these "smart" mice to determine whether the plasticity that operates to guide cortical development is also enhanced and, if so, by which synaptic mechanisms.

Here, we show that plasticity is accelerated in the visual cortex of H-ras^{G12V} mice during the critical period for sensitivity to altered binocular visual experience, and we elucidate the cellular mechanisms involved.

Results

The transgenic mouse line used here expresses H-ras^{G12V} in excitatory neurons at a level similar to that of endogenous H-ras, beginning during the second postnatal week. H-Ras^{G12V} expression occurred in the lateral geniculate nucleus and visual cortex (Fig. S1) and, as described, could be seen in white matter tracts, indicative of presynaptic expression. We found that gross forebrain morphology was normal in H-Ras^{G12V} mice, as described (14). Furthermore, both intrinsic signal imaging and single-unit recordings in H-ras^{G12V} mice revealed normal development of the characteristic, highly specific receptive fields in the mouse visual cortex (Fig. S2 and S3).

NEUROSCIENCE

Accelerated Ocular Dominance Plasticity During the Critical Period in H-ras^{G12V} Mice. We examined ocular dominance plasticity using chronic optical imaging of intrinsic signals in primary visual cortex (V1) during the developmental critical period to measure the magnitude of cortical responses to visual stimuli repeatedly in the same animals before, during, and immediately after MD induced by eyelid suture (9) (Fig. 1*A*). During MD in WT mice, an initial depression of deprived-eye responsiveness was evident after 3 d and was followed by a delayed increase in open-eye responsiveness between 3 and 6 d (Fig. 1 *C–E*). These changes resulted in a shift in the ocular dominance index (ODI), a measure of the relative responsiveness to the two eyes, which was significant after 3 d but not maximal until 6 d of MD in WT mice (Fig. 1*B*). In H-ras^{G12V} mice, the ODI shift occurred much more rapidly (Fig. 1*B*). It was significant after just 1 d (ODI 0.181 ± 0.049 WT vs. 0.078 ± 0.042 H-ras^{G12V}) and became nearly maximal after only 3 d of MD (ODI 0.105 ± 0.023 WT vs. 0.030 ± 0.025 H-ras^{G12V}; Fig. 1*B*). The accelerated OD shift was principally the result of a change in open-eye responsiveness (Fig. 1 *D* and *E*). It was particularly striking that open-eye responsiveness in H-ras^{G12V} mice was highly significantly increased by 3 d of MD, at a time when no change was evident in WT animals (Fig. 1 *D* and *E*).

As in WT mice, the accelerated plasticity in H-ras^{G12V} mice has a clear critical period. Six days of MD beginning between P45 and P48, after the peak of the normal critical period, were required to produce a significant ocular dominance shift, just as in WT animals (ODI shift 0.07 ± 0.02, $P < 0.05$ WT; 0.13 ± 0.03 $P < 0.01$ H-ras^{G12V}; $n = 6$ each). In contrast to findings at the peak of

Author contributions: M.K., C.E.C., A.J.S., M.P.S., and K.F. designed research; M.K., C.E.C., and Y.-S.L. performed research; M.K. and C.E.C. analyzed data; and M.K., C.E.C., A.J.S., M.P.S., and K.F. wrote the paper.

The authors declare no conflict of interest.

[1]M.K. and C.E.C. contributed equally to this work.

[2]To whom correspondence should be addressed. E-mail: stryker@phy.ucsf.edu.

This article contains supporting information online at www.pnas.org/lookup/suppl/doi:10.1073/pnas.1013866107/-/DCSupplemental.

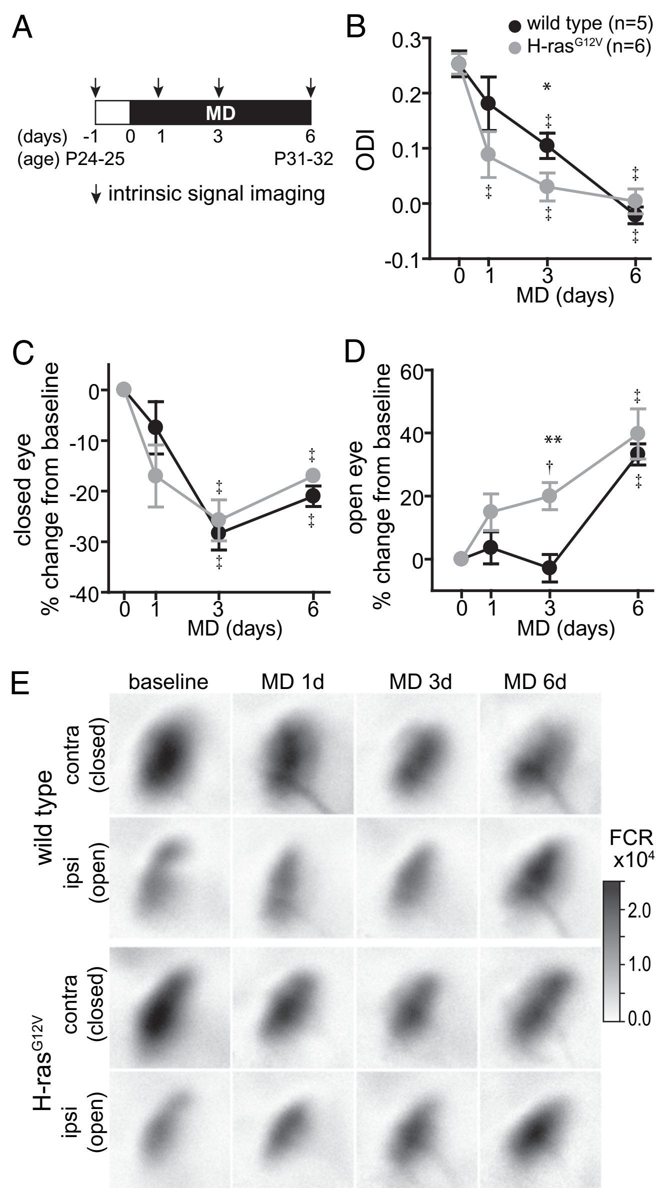

Fig. 1. Repeated imaging of intrinsic signals reveals accelerated in vivo cortical plasticity in H-ras^{G12V} mice during MD. (*A*) Experimental schedule for chronic intrinsic signal imaging. Intrinsic signals were recorded from binocular visual cortex contralateral to the closed eye before (−1), and 1, 3, and 6 d after eyelid suture at day 0. (*B*) Ocular dominance index (ODI) during MD. Data are shown as mean ± SEM: $^{**}P < 0.01$, $^{*}P < 0.05$ H-ras^{G12V} vs. WT, one-way ANOVA followed by multiple comparisons with Bonferroni correction; $^{‡}P < 0.01$, $^{†}P < 0.05$ vs. baseline, repeated measures ANOVA followed by multiple comparisons with Bonferroni correction. (*C*) Percentage change in closed-eye response magnitude. (*D*) Percentage change in open-eye response magnitude. (*E*) Examples of intrinsic signal images recorded before and during MD. FCR, fractional change in reflectance.

the critical period, no significant shift in ODI measured with intrinsic signal imaging was evident after 1 or 3 d of MD in either genotype (ODI shift after 1 d MD: 0.03 ± 0.01 WT, 0.01 ± 0.02 H-ras^{G12V}; after 3 d MD: 0.01 ± 0.01 WT, 0.06 ± 0.04 H-ras^{G12V}; $n = 6$ each; all $P > 0.05$).

Accelerated Recovery of Visual Responses in H-ras^{G12V} Mice. A mechanistically different form of cortical plasticity, which requires signaling through the TrkB neurotrophin receptor (8), occurs when vision is restored after MD. Because H-ras participates in the signaling cascade downstream of TrkB activation (15), we examined whether recovery was also accelerated in H-ras^{G12V} mice (Fig. 2 *A* and *B*). In WT mice, restoring binocular vision (BV) induced recovery within 1 d (ODI baseline: 0.224 ± 0.031; BV: 0.229 ± 0.029; $P > 0.05$), but recovery under reverse occlusion (RO; reopening the deprived eye but closing the previously open eye) was much slower, with only modest recovery after 1 d (Fig. 2*C*; RO: 0.101 ± 0.039, MD: 0.011 ± 0.038; $P < 0.05$; Fig. S4). In contrast, H-ras^{G12V} mice showed full recovery of the ODI after 1 d of either BV or RO (Fig. 2*C*; baseline: 0.257 ± 0.305, BV: 0.249 ± 0.036, $P > 0.05$; baseline: 0.268 ± 0.242, RO: 0.229 ± 0.029, $P > 0.05$). Closer examination of the RO data showed that the responses to both the open and closed eyes were restored to baseline levels within 24 h in H-ras^{G12V} mice (Fig. 2*D*), whereas in WT mice, neither eye's responsiveness recovered. Thus, the cortical plasticity produced by both MD and recovery from MD was significantly accelerated by H-ras^{G12V} expression.

Accelerated Plasticity in Single Neurons in H-ras^{G12V} Mice. We focused our single-unit assays of plasticity on the time points at which our intrinsic signal imaging showed the most pronounced acceleration of plasticity in H-ras^{G12V} mice: after 3 d of MD and after 1 d of recovery with reverse occlusion (RO) following 5 d of MD. We calculated the ODI for each unit exactly as it was calculated for the binocular cortex as a whole when using intrinsic signal imaging: as the difference between the firing rates evoked by an optimal drifting grating presented to the contralateral and ipsilateral eyes divided by the sum of the two eyes' responses.

Plasticity of the single units was strikingly similar to plasticity measured with intrinsic signal imaging, both after MD and after recovery. Fig. 3*A* shows the average ODI of single units for mice that were not deprived (ND), mice after 3 d of MD, and mice after 1 d of recovery from MD (RO). The OD shift after 3 d MD is much greater in H-ras^{G12V} than in WT mice ($P < 0.01$), and the recovery of the ODI after 1 d RO is insignificant in WT but complete in H-ras^{G12V} mice. Cumulative frequency distributions (Fig. S5 and Tables S1 and S2) show that the average changes were characteristic of the population as a whole and were not the result of a few aberrant units. Examining the responses to stimulation of the two eyes separately, open-eye responsiveness was not increased in WT mice after 3 d of MD but was significantly increased in H-ras^{G12V} animals (Fig. 3*B*, MD; Fig. S5 and Tables S1 and S2). Responses to stimulation of the previously closed eye were completely recovered after 1 d of RO in H-ras^{G12V} mice but were unchanged in WT mice (Fig. 3*C*, RO; Fig. S5 and Tables S1 and S2). In summary, single-unit recordings were consistent with findings from intrinsic signal imaging in revealing accelerated plasticity in H-ras^{G12V} mice both during MD and during recovery from deprivation.

Enhanced Spike Timing-Dependent LTP in Vitro in H-ras^{G12V} Mice. To understand the synaptic mechanisms underlying the acceleration of cortical plasticity in H-ras^{G12V} mice, we studied the properties of L2/3 pyramidal neurons in the binocular zone of V1 in acute brain slices by using whole-cell voltage recordings at the peak of the critical period (P26–30). The passive membrane properties and intrinsic excitability of L2/3 pyramidal neurons in H-ras^{G12V} and WT mice were very similar (Fig. S6). The most salient aspect of enhanced plasticity in vivo in H-ras^{G12V} mice is acceleration both of the increase in open-eye responsiveness during MD and of recovery during RO. Therefore, we first focused on LTP in the L4 to L2/3 pathway, a pathway that has been strongly implicated in the expression of experience-dependent plasticity (16, 17). We induced LTP with a spike timing-dependent protocol by pairing postsynaptic spikes in L2/3 pyramidal neurons with stimulation of L4. In WT mice, this protocol produced significant potentiation in 27% of neurons, giving a mean potentiation magnitude of 1.10 ± 0.21 1 h after LTP induction (Fig. 4 *A* and *B*). Com-

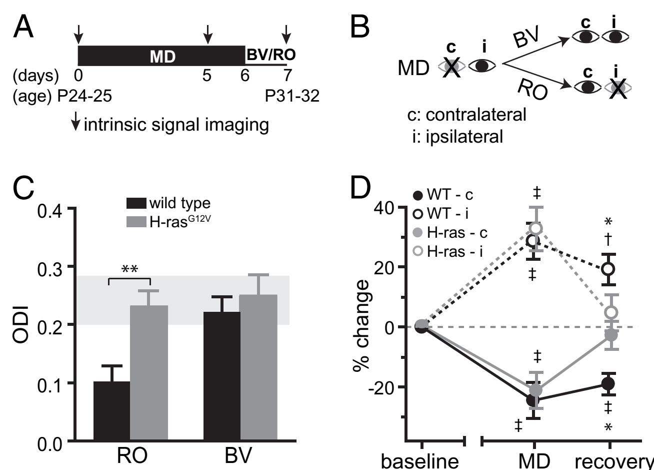

Fig. 2. Accelerated recovery of visual cortical responsiveness after MD in H-ras^{G12V} mice. (*A*) Experimental schedule. (*B*) Schematic of protocols used to induce recovery from the effects of MD. (*C*) ODI after 1 d of recovery. Shaded area represents normal range for ODI. (*D*) Response magnitude evoked by stimulation of the previously deprived eye or previously open eye in mice that have undergone RO after MD. Response magnitude is presented as percentage change from baseline. For all graphs, data are shown as mean ± SEM: $^{**}P < 0.01$, $^{*}P < 0.05$ H-ras^{G12V} vs. WT, one-way ANOVA followed by multiple comparisons with Bonferroni correction; $^{‡}P < 0.01$, $^{†}P < 0.05$ vs. baseline of the corresponding genotype, repeated measures ANOVA followed by multiple comparisons with Bonferroni correction. BV, *n* = 5 each genotype; RO, *n* = 6 each genotype.

parably low rates of successful LTP induction are commonly seen with similar LTP protocols in this pathway (18–20). In striking contrast, LTP was enhanced in H-ras^{G12V} mice, with 60% of neurons showing significant potentiation and a mean potentiation magnitude of 1.56 ± 0.13.

H-ras^{G12V} protein expressed under the CaMKIIα promoter is known to colocalize with endogenous H-ras in axon terminals at CA3 to CA1 synapses (14). Therefore, we next examined short-term synaptic dynamics, which are primarily a presynaptic property (21, 22), at L4 to L2/3 synapses (Fig. 4*C*). In H-ras^{G12V} mice, excitatory postsynaptic potentials (EPSPs) showed pronounced short-term facilitation during eight-pulse stimulus trains, which contrasts with the short-term depression seen at WT synapses (Fig. 4*D*). Greater short-term facilitation is likely to increase summation of postsynaptic responses and, therefore, detection of correlated activity, which is necessary for cortical plasticity. Both presynaptic and postsynaptic mechanisms are known to contribute to cortical LTP (18, 19). We used changes in paired pulse ratio (PPR) to assess the contribution of presynaptic mechanisms to LTP. On average, 1 h after LTP induction, PPR was significantly reduced in H-ras^{G12V} mice (from 1.42 ± 0.08 to 1.15 ± 0.04) but was unchanged in WT mice (from 1.25 ± 0.06 to 1.24 ± 0.14; Fig. 4*E*). Consistent with these changes in PPR, 78% of potentiated neurons in H-ras^{G12V} mice showed a significant reduction in PPR, whereas PPR was not reduced in any of the potentiated neurons in WT mice (Fig. 4*F*). Moreover, potentiation magnitude was strongly correlated with the magnitude of the decrease in PPR after LTP in H-ras^{G12V} mice (Fig. 4*F*). These findings strongly suggest that the LTP enhancement in H-ras^{G12V} mice is predominantly due to a presynaptic mechanism.

Lower Presynaptic Release Probability in H-ras^{G12V} Mice. Greater short-term facilitation suggests that baseline presynaptic release probability is lower at excitatory synapses in H-ras^{G12V} mice than in WT mice (21). To test this hypothesis directly, we measured the rate of use-dependent blockade of NMDARs at L4 to L2/3 excitatory synapses by MK-801, an irreversible open channel blocker (Fig. 5*A*). Use-dependent blockade occurred significantly more slowly in H-ras^{G12V} mice than in WT mice (Fig. 5*B*), with a 3.5-fold greater number of stimuli required to elicit a 50% decrease in response amplitude in H-ras^{G12V} mice (Fig. 5*C*). The mean time constant of the rate of blockade (*SI Materials and Methods*) was also five times longer in H-ras^{G12V} mice (Fig. 5*D*). Analysis of the decay kinetics of NMDAR-mediated responses excluded the possibility that differences in channel open probability could explain the different rates of use-dependent blockade in H-ras^{G12V} and WT mice (Fig. S7). Therefore, presynaptic release probability is reduced at L4 to L2/3 excitatory synapses in H-ras^{G12V} mice.

To determine whether H-ras^{G12V} expression results in a generalized reduction in release probability at all excitatory inputs to L2/3 pyramidal neurons, we measured the frequency of miniature EPSPs (mEPSPs) (Fig. 5*E*), which are thought to result from spontaneous release of single vesicles of neurotransmitter. The frequency of mEPSPs in L2/3 pyramidal neurons was 63% lower in H-ras^{G12V} mice than in WT mice (Fig. 5*F*), consistent with a generalized reduction in release probability at excitatory synapses onto L2/3 pyramidal neurons. In contrast, mEPSP amplitude was identical in WT and H-ras^{G12V} mice (Fig. 5*G*), indicating that postsynaptic response size is unaffected by transgene expression.

mEPSP Frequency Is Affected by Monocular Deprivation in WT and H-ras^{G12V} Mice. We next wished to determine how reduced presynaptic release probability and enhanced LTP in vitro relate to

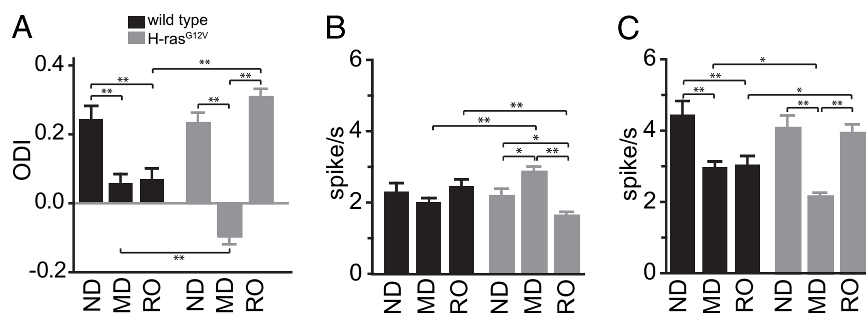

Fig. 3. Plasticity assayed with single-unit recordings is accelerated in H-ras^{G12V} mice. (*A*) ODI calculated as the difference between peak firing rates for ipsilateral (*B*) and contralateral (*C*) responses divided by the sum of the two. (*B*) Firing rates evoked by an optimal drifting grating stimulus presented to the initially open (ipsilateral) eye. (*C*) Firing rates evoked by an optimal drifting grating stimulus presented to the initially deprived (contralateral) eye. ND, no visual deprivation; MD, 3 d of MD; RO, 5 d of MD followed by 1 d of RO. Data are shown in bar graphs as mean ± SEM: $^{*}P < 0.05$, $^{**}P < 0.01$, Mann–Whitney tests in *B* and *C*. $^{*}P < 0.05$, $^{**}P < 0.01$, one-way ANOVA followed by multiple comparisons with Bonferroni correction in *A*. Sample size (units, animal) WT: ND (118, 2), MD (222, 4), and RO (234, 4); H-ras^{G12V}: ND (160, 3), MD (266, 5), and RO (241, 4).

Fig. 4. Enhanced LTP in H-ras^{G12V} mice. (*A*) Temporal profile of EPSP amplitude after LTP induction (black bar) in H-ras^{G12V} (gray) and WT (black) mice. $P < 0.001$, WT vs. H-ras^{G12V}, two-way ANOVA. (*B*) Distributions of normalized EPSP amplitude 1 h after LTP induction. Dashed line indicates threshold for significant potentiation (+≥15%). $n = 15$ per group. (*C*) Example traces showing short-term synaptic dynamics during eight-pulse stimulus trains. (Scale bars: 2 mV; 50 ms.) (*D*) Short-term synaptic dynamics of L4 to L2/3 synapses during eight-pulse stimulus trains. $P < 0.001$ for effect of genotype, two-way ANOVA, $n = 20$ per group. (*E*) Paired pulse ratio (PPR) before ($t_{<0}$) and after ($t_{50–60}$) LTP induction protocol. WT, $P = 0.69$; H-ras^{G12V}, $P = 0.001$ (*), paired *t* tests comparing $t_{<0}$ and $t_{50–60}$. (*F*) Relationship between LTP magnitude and change in PPR for those neurons that showed significant potentiation 1 h after LTP induction. $P = 0.025$, χ^2 test comparing proportions of neurons that showed a significant decrease in PPR after LTP in WT and H-ras^{G12V} mice. Solid gray line indicates linear regression fit for neurons in H-Ras^{G12V} mice ($R^2 = 0.67$, $P = 0.007$). Data are shown as mean ± SEM.

Fig. 5. Reduced presynaptic release probability in H-ras^{G12V} mice. (*A*) Rate of use-dependent blockade of NMDARs by MK-801 for an example neuron from a WT mouse. Double exponential fit (solid black line) and fast- (gray dashed line) and slow- (gray dotted line) component single-exponential functions are shown. (*Inset*) NMDAR-mediated responses to stimulus numbers 1, 5, 10, and 20 for the same neuron. (Scale bars: 1 mV; 20 ms.) (*B*) Rate of use-dependent blockade of NMDARs by MK-801 $P < 0.001$ for WT (black) vs. H-ras^{G12V} (gray) mice at trial 100, Student's *t* test. (*C*) Distribution of the number of stimuli required to induce a 50% block of NMDAR-mediated excitatory neurotransmission. $P = 0.043$, Mann–Whitney test; $P = 0.031$, Kolmogorov–Smirnov test; $n = 10$ per group. (*D*) Distributions of mean time constant of exponential decay for neurons. $P = 0.001$, Mann–Whitney test. (*E*) Example traces showing mEPSPs recorded in undeprived WT (*i*) and H-ras^{G12V} (*ii*) mice. (Scale bars: 0.25 mV; 50 ms.) (*F*) mEPSP frequency before ($n = 15$) or after 3 or 6 d of MD ($n = 20$ per group). Data are shown as mean ± SEM. $P = 0.038$, one-way ANOVA on Ranks; $^*P < 0.05$ WT vs. H-ras^{G12V}; $^\dagger P < 0.05$ between time points. (*G*) mEPSP amplitude before ($n = 15$) or after 3 or 6 d of MD ($n = 20$ per group). Data are shown as mean ± SEM. $P = 0.97$, one-way ANOVA.

the accelerated ocular dominance plasticity that H-ras^{G12V} mice exhibit in vivo. We first considered an experiment to determine whether LTP is occluded by prior MD at ipsilateral (open) eye inputs in H-ras^{G12V} mice. However, in the binocular zone of V1, the amount of ipsilateral eye input varies considerably among L2/3 pyramidal neurons (10–12). Indeed, the information transmitted by an individual L4 to L2/3 synapse depends on the balance of input from the two eyes received by the presynaptic neuron. Therefore, ipsilateral eye inputs to L2/3 pyramidal neurons cannot be studied in isolation. Furthermore, presynaptic LTD is thought to underlie depression of closed-eye inputs (16); therefore, given that most L2/3 pyramidal neurons in the binocular zone are contralaterally dominated, LTP might well be enhanced, rather than occluded, by MD.

Instead, we reasoned that mEPSPs, which sample from a relatively large number of the inputs to each neuron, could provide us with a measure of MD-related changes in presynaptic release. Therefore, we performed 3- or 6-d MDs in WT and H-ras^{G12V} mice and recorded mEPSPs in the binocular zone of brain slices from the hemisphere contralateral to the deprived eye. We found no effect of MD on mEPSP amplitude in WT or H-ras^{G12V} mice (Fig. 5*G*). This finding does not rule out the possibility that changes in postsynaptic responsiveness could have occurred at a subset of inputs to L2/3 pyramidal neurons. Indeed, opposite

changes at contralateral and ipsilateral eye inputs might be expected, which would counteract one another.

In contrast to the lack of effect on mEPSP amplitude, in H-ras^{G12V} mice, mEPSP frequency increased significantly after 3 d of MD and did not increase further after 6 d of MD (Fig. 5*F* and Fig. S8*A*). Therefore, during MD, the time course of changes in mEPSP frequency matched that of changes in open-eye responsiveness (Fig. 1*D*). This similarity supports a presynaptic mechanism for the accelerated increase in open-eye responsiveness that occurs during MD in H-ras^{G12V} mice. In striking contrast, in WT mice, mEPSP frequency decreased after 3 d of MD, returning to baseline levels after 6 d of MD (Fig. 5*F* and Fig. S8*B*). This result is consistent with a decrease in release probability at deprived contralateral eye inputs, followed by a delayed homeostatic increase in release probability at both contralateral and ipsilateral eye inputs. Notably, mEPSP frequency was similar in WT and H-ras^{G12V} mice after 6 d of MD.

Discussion

Acceleration of Multiple Forms of Visual Cortex Plasticity in H-ras^{G12V} Mice. This study has demonstrated that expression of a constitutively active form of H-ras accelerates multiple forms of plasticity in the visual cortex during the normal developmental critical period. This acceleration was observed both at a global level by using intrinsic signal imaging and at the single-unit level with microelectrode recording. During MD, the most pronounced difference between WT and H-ras^{G12V} mice was the faster increase in open-eye responsiveness in excitatory neurons during MD. Recovery of visual responses by RO after MD was also accelerated in H-ras^{G12V} mice: Responses of excitatory neurons to both the originally deprived (contralateral) and originally open (ipsilateral) eyes were restored to their original levels after just 24 h of RO.

Most previous reports of enhanced cortical plasticity have focused on either altering the timing of the developmental critical period or reactivating plasticity in adult animals (5, 23–29). In contrast, we describe enhanced plasticity at a developmental stage when plasticity is already at its peak. To our knowledge, there is no other example of an enhancement of the rate of plasticity during the critical period. Furthermore, H-ras^{G12V} expression is unique in accelerating both deprivation-induced plasticity and recovery from deprivation. Previous studies have shown that these two processes differ mechanistically, involving distinct cellular processes (8, 30, 31). H-ras is known to initiate signaling pathways leading to activation of distinct sets of effector molecules depending on cellular conditions (15), consistent with our finding that constitutive activation of H-ras affects plasticity both during MD and during recovery from deprivation.

Ocular dominance plasticity in H-ras^{G12V} mice, although accelerated, shares many features with the well-known process in WT mice. In particular, it consists of a decrease in responsiveness to the deprived eye and an increase in responsiveness to the open eye, and has a clear critical period. These findings, together with the development of the characteristic, highly specific response properties of visual cortical neurons, suggest that the effect of constitutive activation of H-ras by expression of the H-ras^{G12V} transgene is to enhance normal plasticity rather than to induce some novel ectopic, unregulated, form of plasticity.

Synaptic Mechanisms That May Underlie Ocular Dominance Plasticity During the Critical Period. The faster rate of use-dependent blockade of NMDARs by MK-801, increased short-term facilitation, and reduced mEPSP frequency all indicate that presynaptic release probability is lower at excitatory synapses in H-ras^{G12V} mice than in WT mice. Spike timing-dependent LTP in vitro was also markedly enhanced in H-ras^{G12V} mice; this enhancement resulted primarily from presynaptic potentiation mechanisms. Our data therefore suggest that increases in presynaptic release probability, from a low initial state, mediate enhanced plasticity in vitro in H-ras^{G12V} mice and may do so in vivo as well. Presynaptic mechanisms of potentiation are known to occur in the cortex (18, 19) but are limited if release probability is high. Therefore, by resetting the position of the synapse within its dynamic range, low initial release probability creates the "headroom" necessary for potentiation by a presynaptic mechanism.

We found that mEPSP frequency was increased in L2/3 pyramidal neurons in H-ras^{G12V} mice after 3 d of MD, which suggests that an increase in release probability may underlie the increase in open-eye responsiveness during the first 3 d of MD in H-ras^{G12V} mice. There was no further increase in mEPSP frequency after 6 d of MD in H-ras^{G12V} mice, again consistent with the time course of the increase in open-eye responsiveness in H-ras^{G12V} mice. In contrast, mEPSP frequency decreased strongly after 3 d of MD in WT mice but returned to baseline levels after 6 d of MD. The initial decrease in mEPSP frequency is in agreement with a previous study (32), which showed that 3 d of monocular lid suture decreased mEPSC frequency by 33% in the monocular zone. Moreover, it suggests that release probability decreased during the first 3 d of MD, consistent with the previously reported presynaptic LTD mechanism for closed-eye depression (16). The decrease in mEPSP frequency during MD in WT mice precedes, and therefore may be necessary for, the delayed increase in open-eye responsiveness. Therefore, the low initial mEPSP frequency and release probability in H-ras^{G12V} mice before MD could obviate the requirement for a decrease in release probability and, thereby, enable open-eye responsiveness to increase faster during MD in H-ras^{G12V} mice than in WT mice.

We found no effect of MD on mEPSP amplitude in WT or H-ras^{G12V} mice. This finding does not rule out the possibility that changes in postsynaptic responsiveness had occurred at a subset of inputs to L2/3 pyramidal neurons. However, it does highlight the difficulty in teasing apart the effects of deprivation on contralateral and ipsilateral eye inputs: Most cells receive a mixture of ipilateral and contralateral inputs, and MD would tend to cause plasticity in opposite directions at the two sets of inputs, which may cancel one another out. Consistent with this idea, a modest (11%) reduction in mEPSC amplitude has been reported in the monocular zone following 3 d of monocular lid suture at P18–21 in Long–Evans rats (32). The fact that we did not observe a mEPSP amplitude decrease after MD could be due to the small magnitude of the change, or to experimental differences between studies, such as species, timing of MD, or differences in plasticity processes between the monocular and binocular zones.

Molecular Mechanisms Underlying Accelerated Plasticity During the Critical Period. Signaling cascades that involve H-ras are known to be involved in visual cortex plasticity (for review, see ref. 33). The TrkB neurotrophin receptor, which is activated by BDNF, is one of the upstream activators of H-ras (15). In WT mice, TrkB kinase activity is essential for the recovery of deprived-eye responses after MD is ended (8). BDNF levels and TrkB receptor activity in the visual cortex contralateral to the deprived eye are reduced during MD, and restoration of BDNF levels may take some time after deprivation is ended (34). In H-ras^{G12V} mice, constitutive activation of H-ras may remove the requirement for upstream activation, thereby accelerating recovery of visual responses after MD by bypassing a requirement for BDNF-TrkB signaling.

Extracellular signal-regulated kinase (ERK) is one of the downstream effectors of H-ras and is required both for the ocular dominance shift during MD and for LTP at L4 to L2/3 excitatory synapses (26). The ocular dominance shift during MD consists of multiple, mechanistically distinct processes (9), and it is not known in which of these processes ERK function plays a major role. Visual inputs regulate ERK activation in the visual cortex (35). During MD, overall ERK activation is reduced but ERK nuclear signaling increases (34, 36). Constitutively active H-ras might increase this ERK nuclear signaling during MD,

leading to acceleration of plasticity. In addition, mechanisms similar to those operating during recovery could also be invoked in H-ras^{G12V} mice during MD itself. These mechanisms would operate in parallel with those that are normally invoked during MD but would take effect faster because they are not dependent on upstream activation.

Implications for Disease. Several mental retardation and neuropsychiatric conditions such as Angelman syndrome, Fragile X syndrome, and schizophrenia (37–39) are likely to require therapies that enhance the capacity for synaptic plasticity. This study therefore offers a possible avenue for developing therapies for these conditions. Because H-ras^{G12V} acts presynaptically to enhance plasticity, it should simultaneously affect excitatory and inhibitory circuits, thereby offering a single therapeutic target for manipulation of both critical components of the cortical circuit (28).

Materials and Methods

Full methods are available as *SI Materials and Methods*. Generation of the transgenic mouse line that expresses a constitutively active form of H-ras (H-ras^{G12V}) has been described (14). Transgenic mice were maintained in a C57BL/6N (Taconic) background and crossed with 129/SvEmsJ mice (The Jackson Laboratory) to generate F_1 animals used for experiments. Animal care and use were performed in accordance with the UK Animals (Scientific Procedures) Act 1986 and with the approval of the University of California, San Francisco Institutional Animal Care and Use Committee.

In Vivo Experiments. MD was performed at P24–26, and all recordings were made from the primary visual cortex contralateral to the deprived eye under isoflurane anesthesia preceded by chlorprothixene. Repeated imaging of intrinsic signals and data analyses were performed blind to genotype and as described (9). Extracellular recording, spike sorting, and analyses of response properties of single units were also performed blind to genotype and as described (40).

Acute Slice Electrophysiology. Four hundred micrometer-thick coronal slices containing V1 were prepared from P26-P30 H-Ras^{G12V} mice and WT littermates. Whole-cell voltage recordings of L2/3 pyramidal neurons were made at 35–37 °C, and axons in L4 were stimulated with an extracellular electrode. LTP was induced with a spike timing-dependent protocol consisting of 50 EPSP-AP pairs (+5 ms interval) delivered at 2 Hz and repeated four times at 0.025 Hz. Twenty-hertz stimulation was used to assess short-term dynamics and PPRs. mEPSPs were isolated with 1 μM tetrodotoxin, 100 μM picrotoxin, and 50 μM D-AP5 (all Tocris). The rate of use-dependent blockade of NMDAR-mediated synaptic transmission was determined by adding 10 μM MK-801 to magnesium-free ACSF containing 20 μM CNQX, after baseline recordings were obtained, and fitting a double exponential function to response amplitude over time.

Immunohistochemistry. Coronal brain sections (20 μm thick) were prepared from mutant H-ras^{G12V} and WT littermate mice at P28. Frozen sections were fixed with 4% paraformaldehyde, and endogenous peroxidase activity was quenched by treating with 0.3% H_2O_2 in methanol for 30 min. After blocking in 5% normal rabbit serum in PBS-T (0.1% Triton X-100), sections were incubated with anti-HA antibody (diluted 1:100; Roche Applied Science) for 48 h at 4 °C. A biotinylated rabbit anti-rat antibody (1:500, 1 h at room temperature; Vector Laboratories) was used as a secondary antibody, which was followed by avidin–biotin–peroxidase (Vector Laboratories) treatment for 30 min. The signal was visualized by incubating sections in DAB substrate solution (Vector Laboratories).

ACKNOWLEDGMENTS. We thank A. Ranson for help with monocular deprivations for in vitro experiments, Y. Cai for help with the mice, and Drs. D. Darcy and C. Niell for help with in vivo electrophysiology. This work was supported by National Institute of Mental Health Grant P50-MH0779720 (to A.J.S., K.D.F., and M.P.S.).

1. Buonomano DV, Merzenich MM (1998) Cortical plasticity: From synapses to maps. *Annu Rev Neurosci* 21:149–186.
2. Katz LC, Shatz CJ (1996) Synaptic activity and the construction of cortical circuits. *Science* 274:1133–1138.
3. Antonini A, Stryker MP (1993) Rapid remodeling of axonal arbors in the visual cortex. *Science* 260:1819–1821.
4. Fox K, Wong RO (2005) A comparison of experience-dependent plasticity in the visual and somatosensory systems. *Neuron* 48:465–477.
5. Hensch TK (2005) Critical period plasticity in local cortical circuits. *Nat Rev Neurosci* 6: 877–888.
6. Wiesel TN, Hubel DH (1963) Single-cell responses in striate cortex of kittens deprived of vision in one eye. *J Neurophysiol* 26:1003–1017.
7. Frenkel MY, Bear MF (2004) How monocular deprivation shifts ocular dominance in visual cortex of young mice. *Neuron* 44:917–923.
8. Kaneko M, Hanover JL, England PM, Stryker MP (2008) TrkB kinase is required for recovery, but not loss, of cortical responses following monocular deprivation. *Nat Neurosci* 11:497–504.
9. Kaneko M, Stellwagen D, Malenka RC, Stryker MP (2008) Tumor necrosis factor-alpha mediates one component of competitive, experience-dependent plasticity in developing visual cortex. *Neuron* 58:673–680.
10. Mrsic-Flogel TD, et al. (2007) Homeostatic regulation of eye-specific responses in visual cortex during ocular dominance plasticity. *Neuron* 54:961–972.
11. Gordon JA, Stryker MP (1996) Experience-dependent plasticity of binocular responses in the primary visual cortex of the mouse. *J Neurosci* 16:3274–3286.
12. Dräger UC (1975) Receptive fields of single cells and topography in mouse visual cortex. *J Comp Neurol* 160:269–290.
13. Heynen AJ, et al. (2003) Molecular mechanism for loss of visual cortical responsiveness following brief monocular deprivation. *Nat Neurosci* 6:854–862.
14. Kushner SA, et al. (2005) Modulation of presynaptic plasticity and learning by the H-ras/extracellular signal-regulated kinase/synapsin I signaling pathway. *J Neurosci* 25:9721–9734.
15. Reichardt LF (2006) Neurotrophin-regulated signalling pathways. *Philos Trans R Soc Lond B Biol Sci* 361:1545–1564.
16. Crozier RA, Wang Y, Liu CH, Bear MF (2007) Deprivation-induced synaptic depression by distinct mechanisms in different layers of mouse visual cortex. *Proc Natl Acad Sci USA* 104:1383–1388.
17. Trachtenberg JT, Trepel C, Stryker MP (2000) Rapid extragranular plasticity in the absence of thalamocortical plasticity in the developing primary visual cortex. *Science* 287:2029–2032.
18. Hardingham N, Fox K (2006) The role of nitric oxide and GluR1 in presynaptic and postsynaptic components of neocortical potentiation. *J Neurosci* 26:7395–7404.
19. Sáez I, Friedlander MJ (2009) Plasticity between neuronal pairs in layer 4 of visual cortex varies with synapse state. *J Neurosci* 29:15286–15298.
20. Seol GH, et al. (2007) Neuromodulators control the polarity of spike-timing-dependent synaptic plasticity. *Neuron* 55:919–929.
21. Dobrunz LE, Stevens CF (1997) Heterogeneity of release probability, facilitation, and depletion at central synapses. *Neuron* 18:995–1008.
22. Zucker RS, Regehr WG (2002) Short-term synaptic plasticity. *Annu Rev Physiol* 64: 355–405.
23. Maya Vetencourt JF, et al. (2008) The antidepressant fluoxetine restores plasticity in the adult visual cortex. *Science* 320:385–388.
24. He HY, Hodos W, Quinlan EM (2006) Visual deprivation reactivates rapid ocular dominance plasticity in adult visual cortex. *J Neurosci* 26:2951–2955.
25. He HY, Ray B, Dennis K, Quinlan EM (2007) Experience-dependent recovery of vision following chronic deprivation amblyopia. *Nat Neurosci* 10:1134–1136.
26. Di Cristo G, et al. (2001) Requirement of ERK activation for visual cortical plasticity. *Science* 292:2337–2340.
27. Pizzorusso T, et al. (2002) Reactivation of ocular dominance plasticity in the adult visual cortex. *Science* 298:1248–1251.
28. Morishita H, Hensch TK (2008) Critical period revisited: Impact on vision. *Curr Opin Neurobiol* 18:101–107.
29. Sale A, et al. (2007) Environmental enrichment in adulthood promotes amblyopia recovery through a reduction of intracortical inhibition. *Nat Neurosci* 10:679–681.
30. Liao DS, Mower AF, Neve RL, Sato-Bigbee C, Ramoa AS (2002) Different mechanisms for loss and recovery of binocularity in the visual cortex. *J Neurosci* 22:9015–9023.
31. Krahe TE, Medina AE, de Bittencourt-Navarrete RE, Colello RJ, Ramoa AS (2005) Protein synthesis-independent plasticity mediates rapid and precise recovery of deprived eye responses. *Neuron* 48:329–343.
32. Maffei A, Turrigiano GG (2008) Multiple modes of network homeostasis in visual cortical layer 2/3. *J Neurosci* 28:4377–4384.
33. Tropea D, Van Wart A, Sur M (2009) Molecular mechanisms of experience-dependent plasticity in visual cortex. *Philos Trans R Soc Lond B Biol Sci* 364:341–355.
34. Majdan M, Shatz CJ (2006) Effects of visual experience on activity-dependent gene regulation in cortex. *Nat Neurosci* 9:650–659.
35. Cancedda L, et al. (2003) Patterned vision causes CRE-mediated gene expression in the visual cortex through PKA and ERK. *J Neurosci* 23:7012–7020.
36. Takamura H, Ichisaka S, Hayashi C, Maki H, Hata Y (2007) Monocular deprivation enhances the nuclear signalling of extracellular signal-regulated kinase in the developing visual cortex. *Eur J Neurosci* 26:2884–2898.
37. Ehninger D, Li W, Fox K, Stryker MP, Silva AJ (2008) Reversing neurodevelopmental disorders in adults. *Neuron* 60:950–960.
38. Yashiro K, et al. (2009) Ube3a is required for experience-dependent maturation of the neocortex. *Nat Neurosci* 12:777–783.
39. Bureau I, Shepherd GM, Svoboda K (2008) Circuit and plasticity defects in the developing somatosensory cortex of FMR1 knock-out mice. *J Neurosci* 28:5178–5188.
40. Niell CM, Stryker MP (2008) Highly selective receptive fields in mouse visual cortex. *J Neurosci* 28:7520–7536.